



Majorana bound states in a quantum dot device coupled with a superconductor zigzag chain

Antonio T. M. Beirão¹ · Miraci Silva Costa² · Alexandre de S. Oliveira¹ · Jorsi J. da C. Cunha² · Shirsley S. da Silva³ · Jordan Del Nero^{1,2,4}

Published online: 27 June 2018
© Springer Science+Business Media, LLC, part of Springer Nature 2018

Abstract

Research in condensed matter physics on topological insulators and superconductors has contributed greatly to the characterization of the surface properties and zero modes of nanowires. In this work we investigated theoretically, using the recursive Green's function approach, electron transport through a T-shaped single-level spinless quantum dot, connected to a zigzag chain and coupled to a p -wave superconductor. This model is an extension of the Kitaev chain for a triangular network of finite size with three, four, and five sites. We found that the Majorana zero modes can be tuned through the coupling parameters of the device and that the linear conductance shows Majorana bound states (MBS) in the topological phase, being maximally robust in the general topological phase. This more realistic model permits the detection of MBS via control of the parameters governing the electronic tunneling and could be helpful for relevant experiments.

Keywords Majorana fermions · Recursive Green's function approach · Kitaev chain · Electronic nanodevices · Quantum dot · T-shaped · Qubit · Majorana bound states (MBS)

1 Introduction

Majorana fermions (MFs) are neutral particles that constitute their own antiparticles. Although first proposed to describe fundamental particles [1], they gained importance after Majorana bound states (MBS) were detected. This implies the degeneracy of the fundamental state and allows the system to support excitations with non-Abelian statistics (i.e., particles that are neither fermions nor bosons) [2]. There is currently a significant interest in topological quantum computers [3], which make use of degenerate ground states of topological matter to encode qubits [4].

Experiments with ultracold atoms [5, 6] in optical networks offer great control over both the mobility and the intensity of the interactions of periodic arrangements and have been proposed to detect Majorana fermions using semiconductor wires, topological superconductors, insulators, and magnetic adatoms. Moreover, experimental realization of a proximity-induced topological superconductor was recently reported [7], forming states connected to MBS in InSb nanowires.

The Kitaev chain [8] is a model for detecting Majorana fermions through the MBS located at the ends of a one-dimensional (1D) chain above a topological superconductor of spin-triplet or p -wave type. The superconductor that supports a Majorana fermion must necessarily be topological [9, 10].

The MBS wavefunctions observed experimentally for a long nanowire by Mourik et al. [7] decay exponentially when a large degree of disorder is included in the model [11]. Furthermore, study of finite-length chains is relevant, because they are exactly solvable and MBS are perfectly located at the ends. Moreover, experimentally, long semiconductor nanowires coupled with the surface of a superconductor [12] can basically be considered to be segmented by disorder into a smaller number of coherent chains [7].

✉ Antonio T. M. Beirão
thiago.ppgee.ufpa@gmail.com

¹ Pós-graduação em Engenharia Elétrica, Universidade Federal do Pará, Belém, PA 66075-970, Brazil

² Pós-graduação em Física, Universidade Federal do Pará, Belém, PA 66075-970, Brazil

³ Faculdade de Física, Universidade Federal do Pará, Ananindeua, PA 67030-000, Brazil

⁴ Faculdade de Física, Universidade Federal do Pará, Belém, PA 66075-110, Brazil

A specific type of arrangement with triangular zigzag geometry has been investigated. In this case, adding one or more sites to the zigzag chain produces coupled inverted triangles (chiral modes) [13]. In this work, we consider a zigzag chain and the influence of such a triangular network on the emergence of unpaired Majorana modes, corresponding to a tight-binding representation of a 1D chain above a topological superconductor [13].

The system consists of two leads in contact with a single-level quantum dot (QD) [14], coupled to a nanowire of zigzag atoms above a topological superconductor (TS) with p -wave pairing (Fig. 1a). The QD is a possible candidate for detection of MBS [15–17]. Study of quantum transport through a QD coupled with MBS (QD-MBS) also extends to system configurations based on a T-shaped QD structure [18]. More recently, study of quantum transport through QD-MBS was extended to multi-QD systems [19].

The chemical potential μ , hopping h , and pairing amplitude Δ induce relatively complex couplings; the model illustrated in Fig. 1a is analyzed in two phases: (a) the trivial phase with $\mu < 0$ and $\Delta = h = 0$, and (b) the topological phase with $\mu = 0$ and $\Delta = h \neq 0$, as well as (b.1) the more general topological situation with $\mu \neq 0$ and $\Delta \neq h$, which still lies in the topological phase [2, 13] (Fig. 1c).

In Fig. 1c, the green curve shows the transition between the trivial and topological phases. Any point on this curve corresponds to the system in phase transition, i.e., $E_Z = \sqrt{\Delta^2 + \mu^2}$, where E_Z is the Zeeman energy due to the external magnetic field \mathbf{B} . Below the green curve, the system is represented by the trivial phase with $E_Z < \sqrt{\Delta^2 + \mu^2}$; Above the green curve, the system is characterized by the topological phase (b) with $\mu = 0$, $h_\alpha = \Delta_\alpha = \Delta = h \neq 0$ and by the more general topological situation with $\mu \neq 0$ and $\Delta \neq h$ (b.1), but still in the topological phase.

The model with five sites is investigated based on the phase diagram in Fig. 1d, plotted as pairing amplitude (Δ) versus QD chain coupling (λ). The topological phase is robust and sensitive for $\Delta \approx 0.1$, characterizing the phase transition and ensuring detection of Majorana fermions for $G_C(\omega) = 0.5$.

We carried out calculations at the thermodynamic limit in the context of Green's functions [16, 20], focusing on finite-size effects by varying the free parameters of the model for three, four, and five sites, for further projection of the behavior for n sites. In fact, we performed calculations under conditions of very low temperatures and small potential differences [21], such that the temperature almost does not affect the conductance curve and quantum effects are preserved.

The aim of this work is to consider a more realistic configuration based on the complexity of the triangular network chain (triangular disorder) [22]. This model is an extension of the Kitaev chain [13] and, in addition, is an experimentally realistic example for detection of Majorana fermions [17].

2 Methodology

We consider a single-level quantum dot (QD), in contact with spinless leads, coupled to a nanowire of zigzag atoms formed by two Kitaev chains (with odd or even sites) [13, 22] above a topological superconductor with p -wave pairing.

The system is split into three parts: quantum dot (QD), leads (L), and zigzag chain atoms (C), as shown by the Hamiltonian in Eq. 1.

The Hamiltonian of a finite 1D chain of size L is given by

$$\mathcal{H} = \mathcal{H}_D + \mathcal{H}_L + \mathcal{H}_{DL} + \mathcal{H}_{DC} + \mathcal{H}_C, \quad (1)$$

where $\mathcal{H}_D = \epsilon_d d_0^\dagger d_0$ describes the quantum dot with energy tuned to ϵ_d , $\mathcal{H}_L = \sum_{k\alpha} \epsilon_k c_{k\alpha}^\dagger c_{k\alpha}$ describes the left and right metallic leads with chemical potential $\mu_L = 0$, and $\mathcal{H}_{DC} = \lambda d_0^\dagger c_1 + \lambda c_1^\dagger d_0$ and $\mathcal{H}_{DL} = \sum_{k\alpha} V_{k\alpha} (c_{k\alpha}^\dagger d_0 + d_0^\dagger c_{k\alpha})$ describe the coupling between the QD and the first site of the zigzag chain or leads, respectively. In addition, $V_{k\alpha}$ represents the tunneling between the QD and leads, and $\lambda \geq 0$ the coupling between the QD and the chain.

We consider single-component fermions on a finite 1D chain of size L with Hamiltonian $\mathcal{H}_C = \mathcal{H}_{\alpha=1} + \mathcal{H}_{\alpha=2} + \mathcal{H}_\mu$,

where $\mathcal{H}_\mu = -\mu \sum_{i=1}^L (c_i^\dagger c_i)$ is the number operator, and

$$\mathcal{H}_\alpha = \sum_{i=1}^{L-\alpha} \left(-h_\alpha c_i^\dagger c_{i+\alpha} - h_\alpha c_{i+\alpha}^\dagger c_i + \Delta_\alpha c_i c_{i+\alpha} + \Delta_\alpha c_{i+\alpha}^\dagger c_i^\dagger \right) \quad (2)$$

describes the interactions between electrons at adjacent sites and the interactions due to the proximity of the superconductor to the chain. Moreover, c_i and c_i^\dagger are fermionic operators ($i = 1, 2, \dots, L$), $h_\alpha \geq 0$, and $\Delta_\alpha = |\Delta_\alpha| e^{j\theta_\alpha}$ with $\alpha = 1$ and $\alpha = 2$ representing intersite hopping and the pairing amplitudes of the topological superconductor, respectively; the arbitrary phase is θ , and j is the imaginary complex unit. The pairing amplitude terms in \mathcal{H}_α are obtained using Raman-induced dissociation of Cooper pairs or Feshbach molecules forming a Bardeen–Cooper–Schrieffer (BCS) atomic reservoir [13].

Majorana fermions are represented by ξ_{kl} , where $k = A, B$ through $c_l = e^{-j\theta/2} (\xi_{Bl} + j\xi_{Al})/2$ and $c_l^\dagger = e^{j\theta/2} (\xi_{Bl} - j\xi_{Al})/2$, $l = 0, 1, 2, \dots, N$ (where $l = 0$ is the QD) [8]. The ξ_{kl} satisfy $[\xi_{kl}, \xi_{k'l'}]_+ = 2\delta_{kk'}\delta_{ll'}$ and $\xi_{kl} = \xi_{kl}^\dagger$.

We use the recursive Green's function approach [16, 17, 20], based on Green's functions calculated to describe the configuration indicated in Fig. 1a and the interactions between neighboring sites in the chain as shown in Fig. 2b.

The recursive method was validated by the pioneering work of Meier and Wingreen [23], who applied the Green's function method to a two-terminal system coupled to the

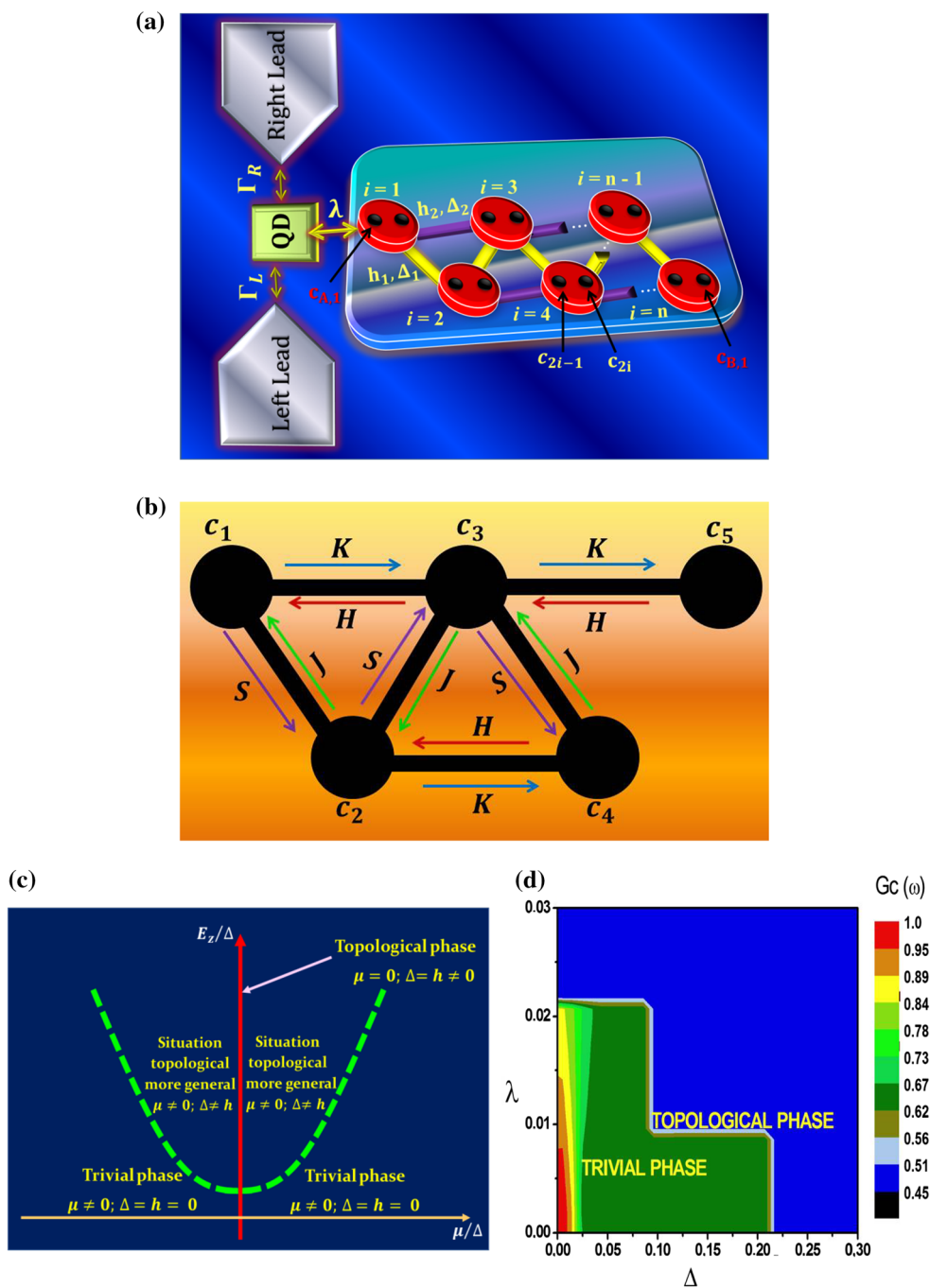


Fig. 1 **a** A quantum dot with single level, coupled with two electrodes, with respective couplings Γ_L and Γ_R , connected to a zigzag chain of atoms with n sites via a coupling constant λ , where the chain is above a superconductor substrate with p -wave pairing. C_{2i-1} and C_{2i} are the Majorana operators for each site. $c_{A,1}$ and $c_{B,1}$ are the MBS at the ends of the 1D chain. The coupling constants within the chain are h_1, Δ_1 and h_2, Δ_2 , called hopping and pairing amplitudes, respectively. **b** The elec-

tronic interaction between the five sites of the zigzag chain, measured by the **K**, **H**, **J**, and **S** coupling matrices. These matrices are presented in Sect. 2 and reveal how much electron tunneling occurs between the sites of the chain. **c** Diagram representing the difference between the trivial and topological phases [2]. **d** Phase diagram $(\Delta) \times (\lambda) \times G_C(\omega)$. The topological phase with Majorana zero modes corresponds to the blue region in the figure for the system containing five sites

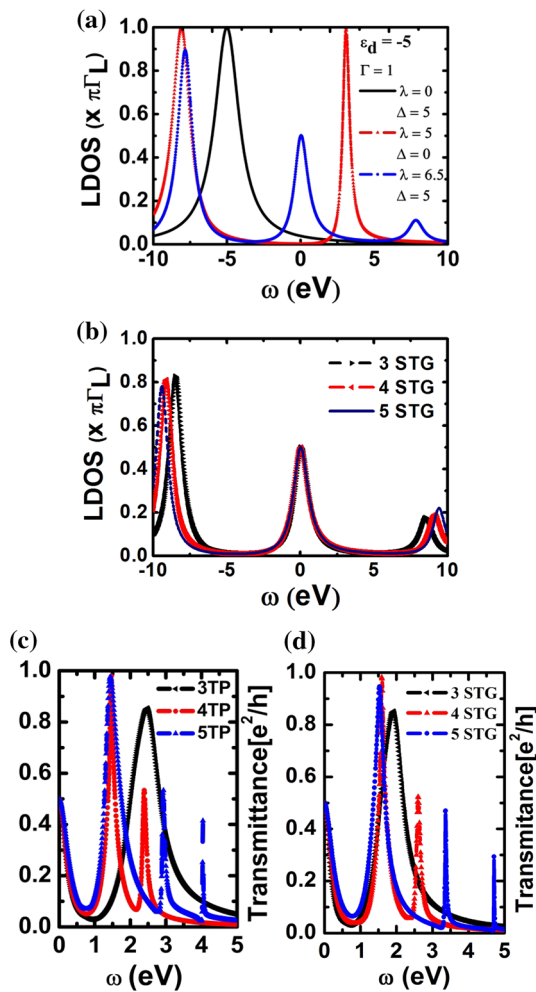


Fig. 2 **a** LDOS with fixed parameters $\epsilon_d = -5$ and $\Gamma_R = \Gamma_L = \Gamma/2$ and coupling between the QD and the chain (λ) and pairing amplitudes (Δ) varying as $\lambda = 0$ and $\Delta = 5$ (black color), $\lambda = 5$ and $\Delta = 0$ (red color), and $\lambda = 6.5$ and $\Delta = 5$ (blue color). **b** LDOS with fixed parameters $\epsilon_d = -5$ and $\Gamma_R = \Gamma_L = \Gamma/2$ in the more general topological situation for three, four, and five sites with parameters tuned to $\epsilon_d = -5$, $\Gamma = 1.2$, and $\Delta_\alpha = 0.2h_\alpha$, and numerically varied λ and h_α . **c** Calculated transmittance in TP ($h_\alpha = \Delta_\alpha = \Delta = h$) with $\epsilon_d = 0$ for: 3TP with parameters $\Gamma = 0.9$, $\lambda = 2.8$, $\Delta = 0.45$; 4TP with $\Gamma = 0.45$, $\lambda = 1.45$, $\Delta = 0.6$; 5TP with $\Gamma = 0.7$, $\lambda = 1.5$, $\Delta = 1.11$. **d** Calculated transmittance in STG ($\mu = 0$ and $h_\alpha \neq \Delta_\alpha$) with $\epsilon_d = 0$ and $\Delta_\alpha = 0.2h_\alpha$ for: 3STG with parameters $\Gamma = 0.7$, $\lambda = 1.7$, $h = 0.175$; 4STG with $\Gamma = 0.43$, $\lambda = 1.6$, $h = 0.325$; 5STG with $\Gamma = 0.52$, $\lambda = 1.45$, $h = 0.65$

central region of a QD. The coupled matrix equations for the topological phase describe the configuration for the model containing n sites (Fig. 1a). The set of the coupled matrix equations for n sites can be represented as

$$\begin{aligned}
 G_n &= \mathbf{H}G_{n-2}, & (3) \\
 G_{n-1} &= \mathbf{H}G_{n-3} + \mathbf{J}G_{n-2}, & (4) \\
 G_{n-2} &= \mathbf{H}G_{n-4} + \mathbf{J}G_{n-3} + \mathbf{S}G_{n-1} + \mathbf{K}G_n, & (5) \\
 &\vdots & \\
 G_3 &= \mathbf{H}G_1 + \mathbf{J}G_2 + \mathbf{S}G_4 + \mathbf{K}G_5, & (6)
 \end{aligned}$$

$$G_2 = \mathbf{J}G_1 + \mathbf{S}G_3 + \mathbf{K}G_4, \tag{7}$$

$$G_1 = \mathbf{Q}G_0 + \mathbf{S}G_2 + \mathbf{K}G_3, \tag{8}$$

$$\mathbf{W}G_0 = \begin{pmatrix} 1 \\ 0 \end{pmatrix} + \mathbf{P}\mathbf{V}G_{k\alpha} + \mathbf{Z}G_1. \tag{9}$$

Therefore, the set of coupled matrix equations for n sites is defined by Eqs. (3)–(9), with

$$\mathbf{H} = \begin{bmatrix} -\frac{\hbar_2}{\omega} & \frac{\Delta_2}{\omega} \\ -\frac{\Delta_2}{\omega} & \frac{\hbar_2}{\omega} \end{bmatrix}; \quad \mathbf{J} = \begin{bmatrix} -\frac{\hbar_1}{\omega} & \frac{\Delta_1}{\omega} \\ -\frac{\Delta_1}{\omega} & \frac{\hbar_1}{\omega} \end{bmatrix}; \quad \mathbf{S} = \begin{bmatrix} -\frac{\hbar_1}{\omega} & -\frac{\Delta_1}{\omega} \\ \frac{\Delta_1}{\omega} & \frac{\hbar_1}{\omega} \end{bmatrix} \tag{10}$$

$$\mathbf{K} = \begin{bmatrix} -\frac{\hbar_2}{\omega} & -\frac{\Delta_2}{\omega} \\ \frac{\Delta_2}{\omega} & \frac{\hbar_2}{\omega} \end{bmatrix}; \quad \mathbf{Q} = \begin{bmatrix} \frac{\lambda}{\omega} & 0 \\ 0 & -\frac{\lambda}{\omega} \end{bmatrix}; \quad \mathbf{Z} = \begin{bmatrix} \lambda & 0 \\ 0 & -\lambda \end{bmatrix}; \tag{11}$$

$$\mathbf{W} = \begin{bmatrix} (\omega - \epsilon_d) & 0 \\ 0 & (\omega + \epsilon_d) \end{bmatrix}; \quad \mathbf{P}\mathbf{V} = \begin{bmatrix} j\Gamma & 0 \\ 0 & j\Gamma \end{bmatrix} \tag{12}$$

such that the matrices \mathbf{H} , \mathbf{J} , \mathbf{S} , and \mathbf{K} represent the values of the pairing amplitudes and hopping for nearest neighbors as well as next nearest neighbors, \mathbf{Q} and \mathbf{Z} show the coupling between the QD and the first site, and \mathbf{W} and $\mathbf{P}\mathbf{V}$ represent the level of the QD and the level broadening between the electrode and the QD, respectively.

We performed calculations to obtain the Green’s function of the model proposed in Fig. 1a for the largest finite quantity desired, as shown by Kraus et al. [13] for a system containing 30 sites and Kraus [22] for a periodic 70×70 lattice.

Based on the set of coupled matrix equations for n sites, we consider the specific case of a zigzag chain with five sites, i.e., $i = 5$ (Eqs. 13–18), for which we have

$$G_5 = \mathbf{H}G_3, \tag{13}$$

$$G_4 = \mathbf{H}G_2 + \mathbf{J}G_3, \tag{14}$$

$$G_3 = \mathbf{H}G_1 + \mathbf{J}G_2 + \mathbf{S}G_4 + \mathbf{K}G_5, \tag{15}$$

$$G_2 = \mathbf{J}G_1 + \mathbf{S}G_3 + \mathbf{K}G_4, \tag{16}$$

$$G_1 = \mathbf{Q}G_0 + \mathbf{S}G_2 + \mathbf{K}G_3, \tag{17}$$

$$\mathbf{W}G_0 = \begin{pmatrix} 1 \\ 0 \end{pmatrix} + \mathbf{P}\mathbf{V}G_{k\alpha} + \mathbf{Z}G_1. \tag{18}$$

Equations (13)–(18) represent the interactions between adjacent sites through the matrices (10) to (12).

Figure 1a and Eq. (14) show the fourth site interacting with the second and third site via the matrices \mathbf{H} and \mathbf{J} that represent the pairing amplitudes of the topological superconductor to the chain and hopping for nearest neighbors as well as next nearest neighbors, respectively.

Using the iterative method to decouple the set of equations (13) to (18), we obtain G'_0 , a 2×1 matrix that represents the Green's function of the QD, given by

$$G'_0 = [W - PV - T_i]^{-1} \begin{pmatrix} 1 \\ 0 \end{pmatrix}, \tag{19}$$

with T_i a 2×2 matrix given by

$$T_i = \begin{bmatrix} R_i(\omega)\lambda^2 & S_i(\omega)\lambda^2 \\ S_i(\omega)\lambda^2 & R_i(\omega)\lambda^2 \end{bmatrix}, \tag{20}$$

and the elements $R_i(\omega)$ and $S_i(\omega)$ of the scattering matrix (20) for $i = 4$ and $i = 5$ sites, respectively, are

$$R_4(\omega) = \frac{(24\Delta^4 - 12\Delta^2\omega^2 + \omega^4)}{48\Delta^4\omega - 16\Delta^2\omega^3 + \omega^5};$$

$$S_4(\omega) = \frac{4\Delta^2(-6\Delta^2 + \omega^2)}{48\Delta^4\omega - 16\Delta^2\omega^3 + \omega^5}, \tag{21}$$

$$R_5(\omega) = \frac{(-32\Delta^6 + 72\Delta^4\omega^2 - 18\Delta^2\omega^4 + \omega^6)}{-64\Delta^6\omega + 96\Delta^4\omega^3 - 20\Delta^2\omega^5 + \omega^7};$$

$$S_5(\omega) = \frac{2\Delta^2(16\Delta^4 - 12\Delta^2\omega^2 + \omega^4)}{-64\Delta^6\omega + 96\Delta^4\omega^3 - 20\Delta^2\omega^5 + \omega^7}, \tag{22}$$

Therefore, inserting Eqs. (20)–(22) into Eq. (19), one obtains the exact Green's function $G^r_{d_0d_0}(\omega)$, according to Ref. [17].

The Green's function of the QD can be expressed as

$$G^r_{d_0d_0}(\omega) = \frac{1}{\omega - \epsilon_d + i\Gamma - R_i(\omega)\lambda^2 \{1 + \lambda^2 \tilde{R}_i(\omega)\}}, \tag{23}$$

with

$$\tilde{R}_i(\omega) = \frac{B_i(\omega)}{\omega + \epsilon_d + i\Gamma - R_i(\omega)\lambda^2} \tag{24}$$

and

$$B_i(\omega) = \frac{S_i^2(\omega)}{R_i(\omega)}. \tag{25}$$

After obtaining $G^r_{d_0d_0}(\omega)$, we detected MBS in the topological phase (TP) and in the more general topological situation (STG, b.1) described in the previous section, and calculated the transmittance $T(\omega)$, conductance $G_C(\omega)$, and local density of states (LDOS) $\rho(\omega)$ of the device containing three, four, and five sites, respectively, where $T(\omega) = G_C(\omega) = -\Gamma \text{Im}\{G^r_{d_0d_0}(\omega)\}$ and $\rho(\omega) = \left(\frac{-1}{\pi}\right) \text{Im}\{G^r_{d_0d_0}(\omega)\}$.

3 Results

According to the formulation described above, we consider symmetric coupling $\Gamma = \Gamma_R = \Gamma_L$ and control the free parameters λ , Δ , and Γ . For a nanowire with three sites, we adjusted the level of the QD to $\epsilon_d = -5$ and varied the parameters Γ , λ , and Δ .

The LDOS in Fig. 2a with $\mu = 0$ and $h_\alpha = \Delta_\alpha = \Delta = h$ corresponds to the topological phase (TP) [2, 13]. The Majorana peak appears at the Fermi level $\epsilon_f = 0$ (blue curve) when the chain is strongly coupled to the QD with $\lambda = 6.5$ and to the superconductor with $\Delta = 5.0$.

In the trivial phase, the red curve with $\lambda = 5$ and $\Delta = 0$ shows a gap at $\omega = 0$, typical of common fermions, and for $\Delta = 0$ and $\lambda = 0$ (black curve), resulting in electron tunneling. Therefore, this T-shaped structure also exhibited nonlocal processes, such as electron tunneling (ET) and Majorana bound states (MBS).

This process extends to the LDOS of the more general topological situation (STG) with $\mu \neq 0$ and $h_\alpha \neq \Delta_\alpha$ (Fig. 2b). In this case, we tuned $\epsilon_d = -5$, $\Gamma = 1.2$, $\Delta_\alpha = 0.2h_\alpha$, with λ and h_α varying to $\lambda = 7.5$ and $h_\alpha = 3.1$ (black color), $\lambda = 8.2$ and $h_\alpha = 3.8$ (red color), and $\lambda = 8.5$ and $h_\alpha = 6.8$ (blue color). This reconfirms the robustness of the MBS for $\omega = 0$, even with the increased complexity of the hopping processes in the chain (Fig. 1b).

Assuming $\epsilon_d = 0$, we obtained the transmittance curves in the TP (Fig. 2c) and STG (Fig. 2d) for chains of 3–5 sites, tuning the remaining parameters to guarantee MBS for $\omega = 0$. By coupling the fourth and fifth sites to the end of the chain, the number of interactions is increased. As a result, the complexity of possible hoppings between sites increases, and new peaks arise.

In both Fig. 2c and d, the largest contribution comes from the first peak adjacent to the MBS, and even in 3STG, this peak shifts to close to the Fermi level.

In Fig. 2d, for STG, a dependence on h was added to the free parameters, and the results again confirm that the topology of the chain created subgaps near the Fermi level, due to the type of coupling between neighboring sites.

In general, the second and third peaks in the STG deviate from the Fermi level, indicating a smaller contribution to the electronic tunneling due to the QD-chain coupling (λ), since the coupling of the superconductor $\Delta_\alpha = 0.2h_\alpha$ is highly sensitive to the topology of the chain.

Figure 3 shows the conductance $G_C(\omega)$ in the more general topological situation. To ensure MBS, the system was tuned to $\epsilon_d = -3$, $\Gamma = 1$, and $\lambda = 8.5\Gamma$, and we varied the hopping couplings with the dependence $h = \Delta/0.2$ for three pairing amplitudes of $\Delta = 0.5$, $\Delta = 1.0$, and $\Delta = 1.5$.

The choice of the pairing amplitudes (Δ) is experimentally based on the technique of Raman-induced dissociation of

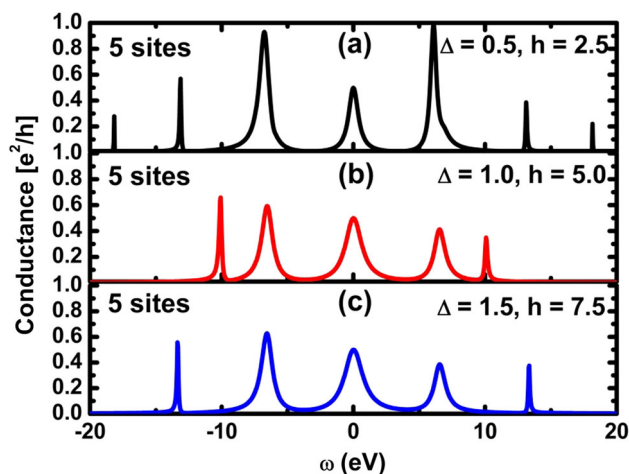


Fig. 3 Conductance of the system in the STG containing five sites with fixed parameters $\varepsilon_d = -3$, $\Gamma = 1$, and $\lambda = 8.5\Gamma$, while varying the pairing amplitudes and hopping to a $\Delta = 0.5$ and $h = 2.5$ (black color), b $\Delta = 1.0$ and $h = 5.0$ (red color), and c $\Delta = 1.5$ and $h = 7.5$ (blue color) (Color figure online)

Cooper pairs or Feshbach molecules forming an atomic BCS reservoir, where μ is the Raman detuning [13].

The best MBS signal was obtained for $\Delta = 0.5$; for $\Delta = 1.5$, MBS were preserved and the highest electron mobility in the chain was guaranteed when $h = 2.5$, in comparison with the linear Kitaev chain.

The choice of the h parameter in our model is experimentally determined by the type of geometry of the studied chain, being related to optical grids that can be obtained using the cold atoms technique [5, 6].

This latter technique allows control of the amplitude of the coupling $h_1 = h_2 = h$ present in the Hamiltonian of the system (Fig. 1a) and thereby the construction of the geometry of the sites in the zigzag chain.

Figure 4 shows the conductance of the model containing five sites for the following parameter values: QD level ε_d , level of the leads Γ , and pairing amplitudes of the topological superconductor Δ , as previously fixed, while varying the hopping h .

Furthermore, we investigated the effect of the dot–chain coupling (λ) with $\varepsilon_d = -1$, $\Delta = 0.5$, and $\Gamma = 1$ for two types of hopping. In Fig. 4a, $h = \Delta/0.1$, while in Fig. 4b, $h = \Delta/0.2$; the nature of the intersite coupling is sensitive to this, while at the same time guaranteeing the MBS at the extremity of the wire.

In Fig. 4a with $h = \Delta/0.1$, the conductance shows two ET peaks, while in Fig. 4b, with $h = \Delta/0.2$, three regular fermion peaks are present. We confirmed the MBS signature, and once again, the hopping value limits the electron mobility in the chain.

In Fig. 4a, b, the fixed values ensure that, when the other parameter values are chosen, only the dot–chain coupling (λ) will vary, guaranteeing the best MBS signal.

A possible experimental technique to study this phenomenon is the mechanical break junction (MBJ) [24–26] in nanowire structures. Indeed, due to the dependence of MBS on λ , it has been shown that MBS can be mechanically modulated in MBJ experiments [27] by changing the distance between the QD and chain.

Figure 5 shows the conductance of the model with five sites. We fixed the level of the QD ε_d , the level of the leads Γ , and the pairing amplitudes Δ . Furthermore, we varied the dot–chain coupling λ and hopping h , respectively.

Figure 5 shows the conductance of the device containing five sites. We tuned $\varepsilon_d = 0$, $\Gamma = 1$, and $\Delta = 2$ and varied the hopping h and dot–chain couplings according to $\lambda = 2h$. For Fig. 5a with $h = 0.4$, we guaranteed ET mobility, but without the presence of MBS.

In Fig. 5b, for $h = 0.6$, we detected, in addition to common fermions at $\omega \cong \pm 4.8, 2.9$, and 1.5 eV, MBS at $\omega = 0$ eV.

The plot in Fig. 5c, for hopping $h = 0.8$, presents an enhanced Majorana signal at $\omega = 0$ together with the signatures of common fermions at $\omega \cong \pm 5.8, 4.2$, and 1.6 eV.

The short-range h interaction affects the detection of MBS, whereas the sufficiently strong long-range interaction induces the appearance of MBS at the extremities of the chain and, therefore, leads to $G_{\text{Peak}} = e^2/2h$, as shown in Fig. 5b, c. Such results indicate the potential to monitor the MBS spectrum in a triangular chain by relating it to experimental techniques applicable to the presented model.

4 Conclusions

We propose a new class of nanodevice using the recursive Green’s function approach that governs the whole model.

The results for the system were analyzed in the trivial phase, the topological phase, and the more general topological situation, for the following parameter values: $\mu \neq 0$, $h_\alpha = \Delta_\alpha = 0$; $\mu = 0$, $h_\alpha = \Delta_\alpha = \Delta = h \neq 0$, and $\mu \neq 0$ and $h_\alpha \neq \Delta_\alpha$, for a finite chain with up to five sites [2, 13].

Was observed a peak in the conductance at $G = e^2/h$ for regular fermions. Furthermore, the peak for Majorana fermions was verified at $G = e^2/2h$.

We confirmed that the zigzag chain topology creates subgaps close to the Fermi level, due to the increased complexity of hopping in the chain for the model with weak disorder, with four and five sites.

These analyses were carried out by choosing values for the free parameters, being experimentally anchored in the type of geometry of the studied chain. This could refer to: (i) an optical grid, which can be produced using the cold atoms technique, or (ii) combination with another technique, such as the mechanical break junction (MBJ) [28] due to the dot–chain interface in the T-shaped geometry [29].

Fig. 4 Conductance of the model containing five sites with fixed parameters and tuned to $\varepsilon_d = -1$, $\Delta = 0.5$, and $\Gamma = 1$. **a** Hopping varying according to $h = \Delta/0.1$, and dot–chain coupling of $\lambda = 3.5$ and $\lambda = 7.5$. **b** Hopping varying according to $h = \Delta/0.2$, and dot–chain coupling of $\lambda = 3.5$ and $\lambda = 6.5$

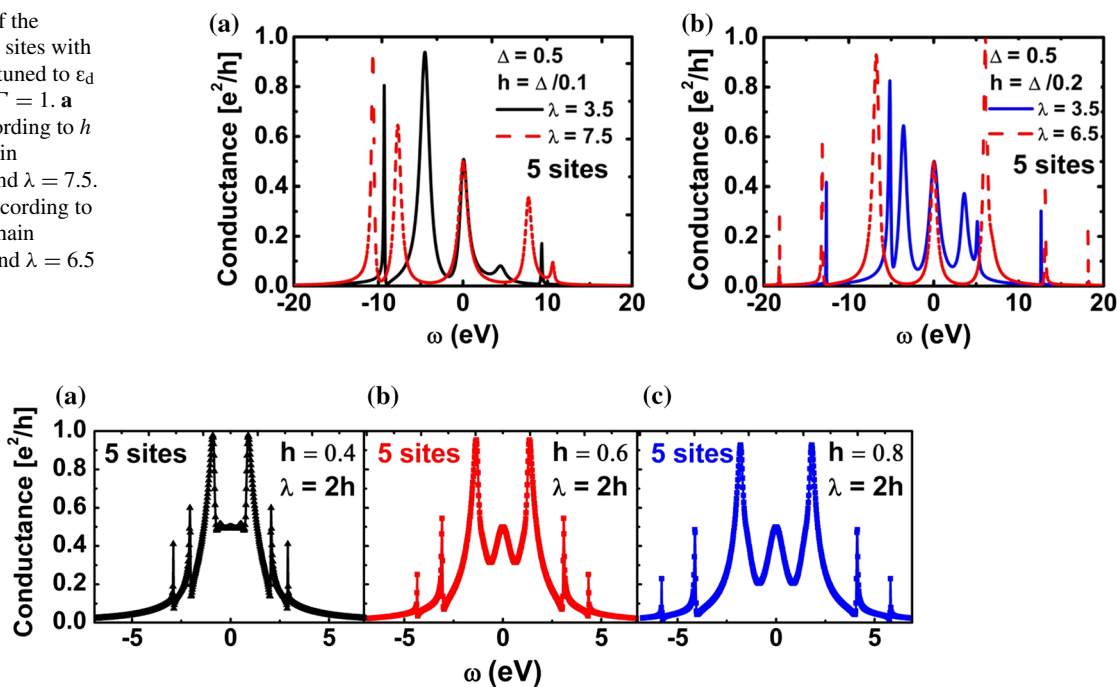


Fig. 5 Conductance of the device containing five sites with parameters tuned and fixed at $\varepsilon_d = 0$ and $\Gamma = 1$ with pairing amplitudes $\Delta = 2$ and **a** hopping of $h = 0.4$ and dot–chain coupling of $\lambda = 2h$, **b** hopping of

$h = 0.6$ and dot–chain coupling of $\lambda = 2h$, and **c** hopping of $h = 0.8$ and dot–chain coupling of $\lambda = 2h$

To decrease the number of interactions between the chain sites and thereby the number of peaks adjacent to the MBS in the zigzag chain of atoms containing five sites, we used the more general topological situation to analyze this effect, with $\mu = 0$ and $h_\alpha = 2, 5\Delta_\alpha$.

The results show that, in the more general topological situation, the effect of disorder in the chain remains for sites 4 and 5.

The effect of disorder in the chain causes fluctuations in the spacing of the levels at the sites, but does not affect the qualitative structure; however, at site 5, Fig. 5a–c shows the elimination of a pair of adjacent peaks at the zero mode.

The results for this more realistic model for obtaining MBS in linear chains, networks, and nanowires are in agreement with literature.

This work represents an analytical and numerical study in systems with experimentally accessible parameter values. We have also shown that it can be applied to systems in which the QDs [30] are defined by other processes, for example, formed by InAs, InSb, or a single nanowire.

Acknowledgements Antonio Thiago Madeira Beirão and Alexandre de Souza Oliveira are grateful to CAPES/FAPESP and CAPES—PROGRAM PRODOUTORAL/UFGA fellowship, respectively. Shirsley S. da Silva and Jordan Del Nero would like to thank CNPq and INCT/Nanomateriais de Carbono for financial support.

References

- Majorana, E.: Teoria simmetrica dell'elettrone e del positrone. *Nuovo Cimento*. **14**, 171–184 (1937). <https://doi.org/10.1007/bf02961314>
- Alicea, J.: New directions in the pursuit of Majorana fermions in solid state systems. *Rep. Prog. Phys.* (2012). <https://doi.org/10.1088/0034-4885/75/7/076501>
- Leijnse, M., Flensberg, K.: Quantum information transfer between topological and spin qubit systems. *Phys. Rev. Lett.* (2011). <https://doi.org/10.1103/physrevlett.107.210502>
- Alicea, J.: Exotic matter: Majorana modes materialize. *Nat. Nanotechnol.* **8**, 623–624 (2013). <https://doi.org/10.1038/nnano.2013.178>
- Jiang, L., et al.: Majorana fermions in equilibrium and in driven cold-atom quantum wires. *Phys. Rev. Lett.* (2011). <https://doi.org/10.1103/physrevlett.106.220402>
- Zhang, C., Tewari, S., Lutchyn, R.M., Das Sarma, S.: $p_x + ip_y$ Superfluid from s-wave interactions of Fermionic cold atoms. *Phys. Rev. Lett.* (2008). <https://doi.org/10.1103/physrevlett.101.160401>
- Mourik, V., Zuo, K., Frolov, S.M., Plissard, S.R., Bakkers, E.P.A.M., Kouwenhoven, L.P.: Signatures of Majorana fermions in hybrid superconductor-semiconductor nanowire devices. *Science* **336**, 1003–1007 (2012). <https://doi.org/10.1126/science.1222360>
- Kitaev, AYu.: Unpaired Majorana fermions in quantum wires. *Phys. Usp.* **44**, 131–136 (2001). <https://doi.org/10.1070/1063-7869/44/10S/S29>
- Sato, M., Ando, Y.: Topological superconductors: a review. *Rep. Prog. Phys.* (2017). <https://doi.org/10.1088/1361-6633/aa6ac7>
- Qi, X.-L., Zhang, S.-C.: Topological insulators and superconductors. *Rev. Mod. Phys.* (2011). <https://doi.org/10.1103/revmodphys.83.1057>

11. Kraus, Y.E., Auerbach, A., Fertig, H.A., Simon, S.H.: Majorana fermions of a two dimensional $p_x + ip_y$ superconductor. *Phys. Rev. B*. (2009). <https://doi.org/10.1103/physrevb.79.134515>
12. De Gennes, P.G.: Boundary effects in superconductors. *Rev. Mod. Phys.* (1964). <https://doi.org/10.1103/revmodphys.36.225>
13. Kraus, C.V., Diehl, S., Zoller, P., Baranov, M.A.: Preparing and probing atomic Majorana fermions and topological order in optical lattices. *New J. Phys.* (2012). <https://doi.org/10.1088/1367-2630/14/11/113036>
14. Law, K.T., Lee, P.A., Ng, T.K.: Majorana fermion induced resonant Andreev reflection. *Phys. Rev. Lett.* (2009). <https://doi.org/10.1103/physrevlett.103.237001>
15. Leijnse, M., Flensberg, K.: Scheme to measure Majorana fermion lifetimes using a quantum dot. *Phys. Rev. B* (2011). <https://doi.org/10.1103/physrevb.84.140501>
16. Vernek, E., Penteado, P.H., Seridonio, A.C., Egues, C.: Subtle leakage of a Majorana mode into a quantum dot. *Phys. Rev. B* (2014). <https://doi.org/10.1103/physrevb.89.165314>
17. Liu, D.E., Baranger, H.U.: Detecting a Majorana-fermion zero mode using a quantum dot. *Phys. Rev. B* (2011). <https://doi.org/10.1103/physrevb.84.201308>
18. Benito, M., Platero, G.: Floquet Majorana fermions in superconducting quantum dots. *Physica E: Low Dimens. Syst. Nanostruct.* (2015). <https://doi.org/10.1016/j.physe.2015.08.030>
19. Li, Z.-Z., Lam, C.-H., You, J.Q.: Probing Majorana bound states via counting statistics of a single electron transistor. *Sci. Rep.* (2015). <https://doi.org/10.1038/srep11416>
20. Xue, Y., Datta, S., Ratner, M.A.: First-principles based matrix-Green's function approach to molecular electronic devices: general formalism. *Chem. Phys.* (2002). [https://doi.org/10.1016/s0301-0104\(02\)00446-9](https://doi.org/10.1016/s0301-0104(02)00446-9)
21. Gong, W.-J., Zhang, S.-F., Li, Z.-C., Yi, G., Zheng, Y.-S.: Detection of a Majorana fermion zero mode by a T-shaped quantum-dot structure. *Phys. Rev. B*. (2014). <https://doi.org/10.1103/PhysRevB.89.245413>
22. Kraus, Y.E., Stern, A.: Majorana fermions on a disordered triangular lattice. *New J. Phys.* (2011). <https://doi.org/10.1088/1367-2630/13/10/105006>
23. Kadanoff, L.P., Baym, G.: *Quantum Statistical Mechanics: Green's Function Methods in Equilibrium and Nonequilibrium Problems*, 1st edn. W.A. Benjamin, Reading (1962)
24. Smit, R.H.M., Noat, Y., Untiedt, C., Lang, N.D., van Hemert, M.C., Ruitenbeek, J.M.: Measurement of the conductance of a hydrogen molecule. *Nature* **419**, 906–909 (2002). <https://doi.org/10.1038/nature01103>
25. Reichert, J., Ochs, R., Beckmann, D., Weber, H.B., Mayor, M., Loehneysen, H.: Driving current through single organic molecules. *Phys. Rev. Lett.* (2002). <https://doi.org/10.1103/physrevlett.88.176804>
26. Wang, L., Ling, W., Zhang, L., Xiang, D.: Advance of mechanically controllable break junction for molecular electronics. *Top. Curr. Chem.* (2017). <https://doi.org/10.1007/s41061-017-0149-0>
27. Perrin, M.L., Verzijl, C.J.O., Martin, C.A., Shaikh, A.J., Eelkema, R., van EschJan, H., van Ruitenbeek, J.M., Thijsen, J.M., van der Zant, H.S.J., Dulic, D.: Large tunable image-charge effects in single-molecule junctions. *Nat. Nanotechnol.* **8**, 282–287 (2013). <https://doi.org/10.1038/nnano.2013.26>
28. Caussanel, M., Schrimpf, R.D., Tsetseris, L., Evans, M.H., Pantelides, S.T.: Engineering model of a biased metal–molecule–metal junction. *J. Comput. Electron.* **6**, 425–430 (2007). <https://doi.org/10.1007/s10825-007-0151-9>
29. Walus, K., Karim, F., Ivanov, A.: Architecture for an external input into a molecular QCA circuit. *J. Comput. Electron.* **8**, 35–42 (2009). <https://doi.org/10.1007/s10825-009-0268-0>
30. Roloff, R., Wenin, M., Pötz, W.: Control strategies for semiconductor-quantum-dot-based single and double qubits. *J. Comput. Electron.* **8**, 29–34 (2009). <https://doi.org/10.1007/s10825-009-0267-1>